

Investigation of ${}^6\text{Li}$ -induced reactions from 54 to 99 MeV on Pd targets

C. M. Castaneda, H. A. Smith, Jr., T. E. Ward, and T. R. Nees

Indiana University Cyclotron Facility and Physics Department, Bloomington, Indiana 47401

(Received 31 May 1977)

Residual decay and in-beam γ -ray data from the bombardment of ${}^{104,106}\text{Pd}$ by ${}^6\text{Li}$ have been acquired at energies of 54, 66, 77, 84, 91, and 99 MeV. Isotopic yields have been determined. The data indicate that substantial pre-equilibrium nucleon emission is present in addition to the usual fusion-evaporation mechanism. The data also suggest the occurrence of the binary breakup of the ${}^6\text{Li}$ accompanied by fragment-induced reactions.

NUCLEAR REACTIONS ${}^{104,106}\text{Pd}({}^6\text{Li}, xny\beta\gamma)$, enriched targets, $E = 54\text{--}99$ MeV; measured in-beam, decay γ rays. Deduced In, Cd, Ag isotopic yields. Geometry-dependent hybrid model; α -d breakup of ${}^6\text{Li}$.

I. INTRODUCTION

Investigation of the excitation functions for ${}^6\text{Li}$ -induced reactions is essential groundwork for their use in the in-beam spectroscopic study of nuclei far from the β -stability valley. In addition, a great deal can be learned about the dominant reaction mechanisms from such studies. In particular, one can study the extent to which the conventional fusion-evaporation behavior of the nuclear reaction, as well as the pre-equilibrium nucleon emission processes, play a role in the overall production of isotopes from ${}^6\text{Li}$ bombardments. Generally the structure of the beam projectile plays a relatively minor role in such investigations of isotope production and is usually not taken into account; but with the ${}^6\text{Li}$ projectile, such an approach is not justified. The pronounced cluster structure of the lithium nucleus enriches the problem and requires that analyses of these reactions include the consideration of projectile behavior and its influence in opening up additional reaction channels. In the present investigation, ${}^{104,106}\text{Pd}$ targets were bombarded with ${}^6\text{Li}$ in the beam energy range of 54 to 99 MeV, and the isotopic yields were determined. From these data we have constructed a general picture of the isotopic distribution of the production cross section and have observed evidence that breakup of the ${}^6\text{Li}$ projectile accompanied by fragment-induced reactions plays a role in determining the ultimate distribution of products from ${}^6\text{Li}$ bombardment. Furthermore, the data discussed below show clearly that pre-equilibrium emission of nucleons is an important feature of the reaction process in this energy range. (This paper presents results, a preliminary report of which was presented earlier.¹)

II. EXPERIMENTAL DETAILS

Beams of ${}^6\text{Li}^{++}$ were obtained from the variable-energy sector-focused cyclotron at the Indiana

University cyclotron facility (IUCF). Lithium beams of energies of 99, 91, 84, 77, 66, and 54 MeV were obtained directly from the accelerator without the use of degrader foils. Ion currents on target were in the range of 0.1 to 5.0 electrical nanoamperes (e nA), with typical values being approximately 0.5 e nA. The beam microstructure consisted of charge bursts approximately 0.5 nsec in duration arriving on target every 30–35 nsec.

The targets irradiated were thin foils of palladium metal, enriched to greater than 95% in ${}^{104,106}\text{Pd}$. The raw material was obtained as enriched metal powder from the Separated Isotopes Division of the Oak Ridge National Laboratory. The powder samples were annealed and rolled into self-supporting foils in the IUCF target preparation laboratory. A summary of the properties of the target materials used in this experiment is given in Table I. The thicknesses of the target foils were determined by measurement of the amount of energy degradation of known α -particle groups from a ${}^{212}\text{Po}$ source. Furthermore, when in the bombardment position, the targets were oriented at an angle of 45° with respect to the beam axis, making the effective target thicknesses in each case $\sqrt{2}$ times the values given in Table I.

Integration of the beam current during bombardment was accomplished by means of a longitudinally segmented Faraday cup. The current outputs of all of the sections were summed and the total was integrated electronically. The digital output of the integrator was used both to drive a scaler and to trigger a pulser; and the output of the latter was introduced into the γ -ray spectra through the test input of the detector preamplifier. In this way, a peak in the γ -ray spectrum was present whose area, compared with the integrator scaler reading, revealed the extent of dead-time losses in the electronics.

The possibility of incomplete charge collection

TABLE I. Summary of enriched Pd targets used in the present experiment.

Isotope	Enrichment (%)	Target thicknesses used (mg/cm ²)
¹⁰⁴ Pd	95.25	14.8, 3.91
¹⁰⁶ Pd	98.48	15.9, 4.35

in the Faraday cup due to multiple scattering in the target was explored in two ways. First, at beam energies of 91 and 66 MeV the γ -ray yields from selected final nuclei were measured with both thicknesses of the ¹⁰⁶Pd target and also with two thicknesses of a ¹⁹⁷Au target (8 mg/cm² and 1 mg/cm²). The measured γ -ray yields per unit of beam charge for both elements were found to scale with target thickness. Under the assumption that multiple scattering losses were negligible with the thin targets, these results were interpreted to mean that such effects could be neglected with the thicker targets as well. A second test of possible multiple scattering effects was performed by measuring the beam currents on the three separate longitudinal sections of the Faraday cup. It was observed that, even at the lowest beam energy (55 MeV) and with the thick ¹⁹⁷Au target, all of the beam was concentrated on the two deepest sections of the cup, with no observable current on the section nearest the entrance aperture to the cup. Thus, it was concluded that all of the beam charge was collected by the Faraday cup assembly, and corrections to the integrated charge for losses from multiple scattering in the targets were not necessary.

The in-beam γ -ray spectra were acquired with the use of a 30.0-cm³ coaxial Ge(Li) detector whose energy resolution under the experimental conditions was measured to be approximately 2.5 keV at 1 MeV. The detector axis was oriented at 90° to the beam direction, and the detector front face was located approximately 3.5 cm from the center of the target foil. A schematic drawing of the experimental setup, including a block diagram of the electronics, is shown in Fig. 1. Spectra of γ rays in prompt coincidence with the beam bursts and interbeam-burst (delayed) γ rays were recorded separately. The distinction between prompt and delayed γ rays was made by observing simultaneously the γ -ray energy and its time distribution with respect to a reference pulse provided by the cyclotron rf synthesizer. This time distribution was measured with a standard time-to-pulse-height converter (TPHC) whose start signal was the γ -ray energy pulse and whose stop signal was the rf pulse. Each γ -ray pulse and its

corresponding TPHC signal was analyzed as a single event. The pulses were received by a Tennelec PACE-CAMAC interface system and subsequently analyzed by the IUCF data acquisition software (DERIVE; see description in Ref. 2). Software gates were set on the prompt and off-prompt regions of the TPHC spectrum, and the γ -ray pulses were stored as prompt or delayed events on the basis of these gates (see Fig. 1). Event rates in the range of 1000–4000 counts/sec were handled by the system with only 10–15% dead-time losses. The timing resolution was measured to be approximately 5 nsec.

Short-lived residual activity spectra were obtained *in situ* with the same data acquisition hardware and software mentioned above, except that ungated γ -ray spectra were analyzed. Residual activity measurements commenced within 30 sec after cessation of bombardment and continued for approximately 15 min. Subsequently, the targets were removed from the bombardment chamber and counted off line for approximately 1 h. The detector used in the off-line measurements was a 25.4-cm³ Ge(Li) coaxial detector with energy resolution of 1.8 keV at 1.1 MeV, and data were acquired with a conventional pulse-handling and multichannel analyzer system.

The isotopes produced in these bombardments were identified by their known in-beam γ rays or by their known decay γ rays and half-lives; and both types of data were used where possible. For determination of production cross sections, greater emphasis was placed in the decay data because of the more reliable knowledge of the γ -ray branching ratios. The energy-dependent absolute detection efficiencies of the off-line and in-beam γ -ray detectors were determined by counting an intensity-calibrated multiple γ -ray source in the experimental geometries. In all cross-section calculations, the usual corrections for target angle and enrichment, dead-time losses, Faraday cup leakage, and composite production of a species by both reactions and decay were made.

III. RESULTS AND DISCUSSION

The measured excitation functions for the ⁹Li-induced reactions on ^{104,106}Pd targets are given in Fig. 2 and presented numerically in Table II. All production cross sections are quoted with a 25% uncertainty, which is a conservative estimate of the combined uncertainties from fitted γ -ray peak areas, beam charge integration, target thickness measurements, and knowledge of γ -ray branching ratios.

It is important to study these data with a view towards understanding which reaction mechanisms

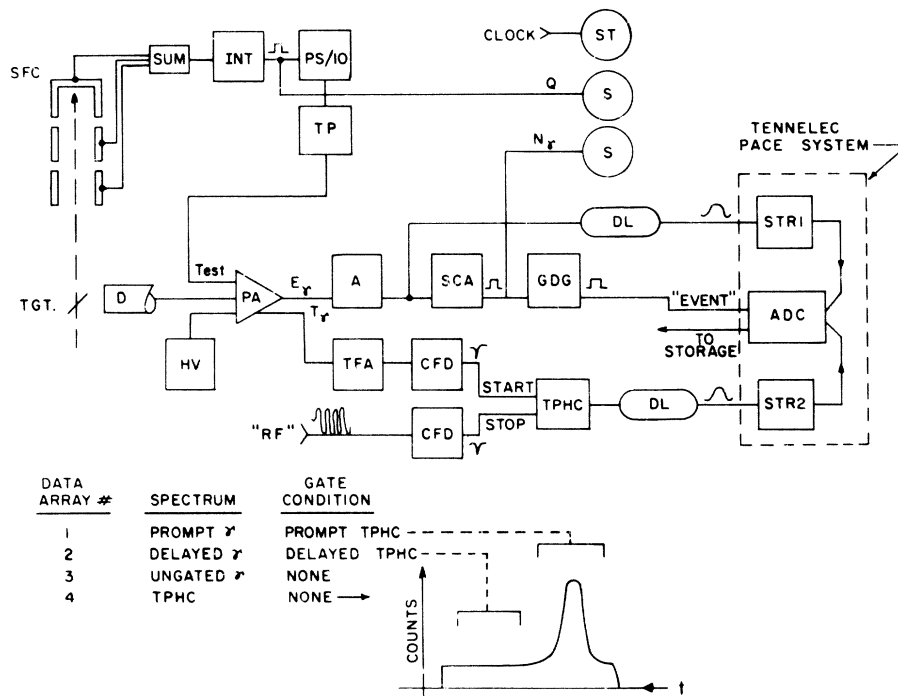


FIG. 1. Schematic block diagram of in-beam data acquisition electronics. Abbreviations used are SFC: segmented Faraday cup; INT: current integrator; PS/10: 1/10 prescaler; TP: triggered pulser; ST: scaler-timer; S: scaler; D: Ge(Li) detector; PA: preamplifier; A: spectroscopy amplifier; SCA: single-channel analyzer; GDG: gate and delay generator; DL: electronic delay; TFA: timing filter amplifier; CFD: constant-fraction discriminator; TPHC: time-to-pulse-height converter; HV: high-voltage power supply; RF: cyclotron rf synthesizer; STR: stretcher; ADC: analog-to-digital converter.

are prevalent in ${}^6\text{Li}$ -induced reactions in the 50–100-MeV energy range. No doubt compound-nucleus processes occur, and it would also be reasonable to anticipate some effects from pre-equilibrium emission of nucleons by the complex (i.e., target + ${}^6\text{Li}$) system. In addition, in view of the well-known α - d and ${}^3\text{He}$ - t cluster structure of ${}^6\text{Li}$, it is likely that there will exist some effects associated with interactions involving one of the ${}^6\text{Li}$ cluster substructures instead of the entire projectile.

The primary theoretical framework in which we will discuss the present results will be that of the geometry-dependent hybrid model (GDHM),³⁻⁷ which describes the time evolution of nuclear reactions by means of compound-nuclear evaporation and pre-equilibrium nucleon emission processes. A GDHM calculation uses the exciton formalism of Griffin,⁸ combined with the more detailed master equation approach of Harp, Miller, and Berne,^{9,10} and takes into account the variation of the nuclear density along the path of the incoming projectile.¹¹ This approach has been applied extensively in proton- and α -induced reactions (see, e.g., Refs. 7, 12, and other references cited in Ref. 12). One of the more important in-

put parameters to these calculations is the initial number of excitons (N_0) in the target + projectile system. Generally, with even-even targets, the best results are obtained when N_0 is chosen to be equal to the number of nucleons in the projectile, with the neutron and proton excitons being distributed the same way that the neutrons and protons are distributed in the incident projectile.⁴ In the case of ${}^6\text{Li}$ -induced reactions on even Pd targets, our best value of N_0 was 6 (three protons and three neutrons). A further approximation, utilized in this GDHM calculation and known as the s -wave approximation,^{13,14} imposes the assumption that the rotational energy brought in by an incident projectile with nonzero impact parameter manifests itself solely as an increase in the angular momentum of the target-projectile system without contributing to the "thermal" energy of that system. This "thermal" energy is that which is available to evaporate nucleons or give rise to pre-equilibrium emission and is assumed to come from either that fraction of the target-projectile interactions in which the two constituents are in a relative s state or the *internal* excitation which occurs in the fusion of target and projectile in states of nonzero angular momentum.

TABLE II. Summary of the measured production cross sections for ${}^6\text{Li}$ on ${}^{106}\text{Pd}$ (upper entry for each product) and ${}^{104}\text{Pd}$ (lower entry). Cross sections are in millibarns and are quoted with a 25% uncertainty.

Reaction product	Reaction ^a	$E\gamma$ ^b	BR ^c	$E(\text{Li})$ (MeV)					
				54	66	77	84	91	99
${}^{108}\text{In}$	$({}^6\text{Li}, 4n)$	875	0.85	127	37	18	9	3	5
	$({}^6\text{Li}, 2n)$			4					
${}^{107}\text{In}$	$({}^6\text{Li}, 5n)$	205	0.485	158	120	46	27	33	14
	$({}^6\text{Li}, 3n)$			23	9	4	3		
${}^{106}\text{In}$	$({}^6\text{Li}, 6n)$	861	0.69		45	31		19	
	$({}^6\text{Li}, 4n)$			112		50	47		19
${}^{105}\text{In}$	$({}^6\text{Li}, 7n)$	131	0.5			5		5	
	$({}^6\text{Li}, 5n)$			36		31			
${}^{109}\text{Cd}$	$({}^6\text{Li}, p2n)$	522*	0.9	70					
	$({}^6\text{Li}, p)$	836*	0.75						
${}^{108}\text{Cd}$	$({}^6\text{Li}, p3n)$			313	133	52	48	18	
	$({}^6\text{Li}, pn)$	875*	1.0						
${}^{107}\text{Cd}$	$({}^6\text{Li}, p4n)$			458	507	435	190	273	100
	$({}^6\text{Li}, p2n)$	93	0.048	130					
${}^{106}\text{Cd}$	$({}^6\text{Li}, p5n)$	861*	1.0	35	140	215	230	218	244
	$({}^6\text{Li}, p3n)$			553	255	128	56	55	15
${}^{105}\text{Cd}$	$({}^6\text{Li}, p6n)$						102	133	172
	$({}^6\text{Li}, p5n)$			264	280	224	111	119	45
${}^{104}\text{Cd}$	$({}^6\text{Li}, p7n)$						4	20	27
	$({}^6\text{Li}, p5n)$	83	0.79	0.6	70	203	110	153	80
${}^{103}\text{Cd}$	$({}^6\text{Li}, p8n)$								
	$({}^6\text{Li}, p6n)$					11	57	39	32
${}^{107}\text{Ag}$	$({}^6\text{Li}, 2p3n)$	866* ^d		31					
	$({}^6\text{Li}, 2pn)$	648*	1.0						
${}^{106}\text{Ag}$	$({}^6\text{Li}, 2p4n)$			40	30		13		4
	$({}^6\text{Li}, 2p2n)$	110* ^e	0.61	16					
${}^{105}\text{Ag}$	$({}^6\text{Li}, 2p5n)$	864*		209	147	114	154	150	283
	$({}^6\text{Li}, 2p3n)$	165*	1.0	134	176	164	156	145	62
${}^{104}\text{Ag}$	$({}^6\text{Li}, 2p6n)$	857	0.99	49	79	100	55	42	100
	$({}^6\text{Li}, 2p4n)$	768	0.66	130	150	460	210		200
${}^{103}\text{Ag}$	$({}^6\text{Li}, 2p5n)$	118	0.28		17	80		41	48
	$({}^6\text{Li}, 2p5n)$	148	0.23	116	117	246	173		245
${}^{102}\text{Ag}$	$({}^6\text{Li}, 2p8n)$					11		63	26
	$({}^6\text{Li}, 2p6n)$	719	0.28	31	75	107	29		56
${}^{101}\text{Ag}$	$({}^6\text{Li}, 2p9n)$								
	$({}^6\text{Li}, 2p7n)$	261	1.0			13			

^a The reaction is designated as $({}^6\text{Li}, \nu p \nu n)$, even though the possibility exists that $({}^6\text{Li}, d \nu n)$ and $({}^6\text{Li}, \alpha \nu n)$ will contribute to the observed production.

^b The energy in keV of the γ ray used to identify the reaction product. Generally, decay data were used to fix the scale of the cross section since γ -ray branching ratios are better known in such cases. However, some cross sections were determined solely from in-beam γ -ray intensities, and in these cases the energy of the γ ray used in the identification is flagged with an asterisk (*).

^c Branching ratios of the identification γ ray, expressed as the number of photons per β disintegration of the product, or (in the case of in-beam γ rays) the number of photons per nuclide produced in beam.

^d γ -ray data from Ref. 36.

^e Intensities taken from $(\alpha, \nu n \gamma)$ work in Ref. 37.

It is evident from Fig. 2 that the ${}^6\text{Li}$ -induced reactions on ${}^{104,106}\text{Pd}$ are dominated by Cd and Ag production, which can be partially understood as the result of the increasing probability for charged-particle emission by nuclei on the neutron-deficient side of the β -stability line. In fact,

our GDHM calculations predict large cross sections for the $({}^6\text{Li}, p \nu n) + ({}^6\text{Li}, d \nu n)$ and $({}^6\text{Li}, 2p \nu n) + ({}^6\text{Li}, \alpha \nu n)$ processes compared with the $({}^6\text{Li}, \nu n)$ yield in this mass region.

Our data in fact demonstrate that ${}^6\text{Li}$ -induced reactions not only proceed by a fusion-evaporation

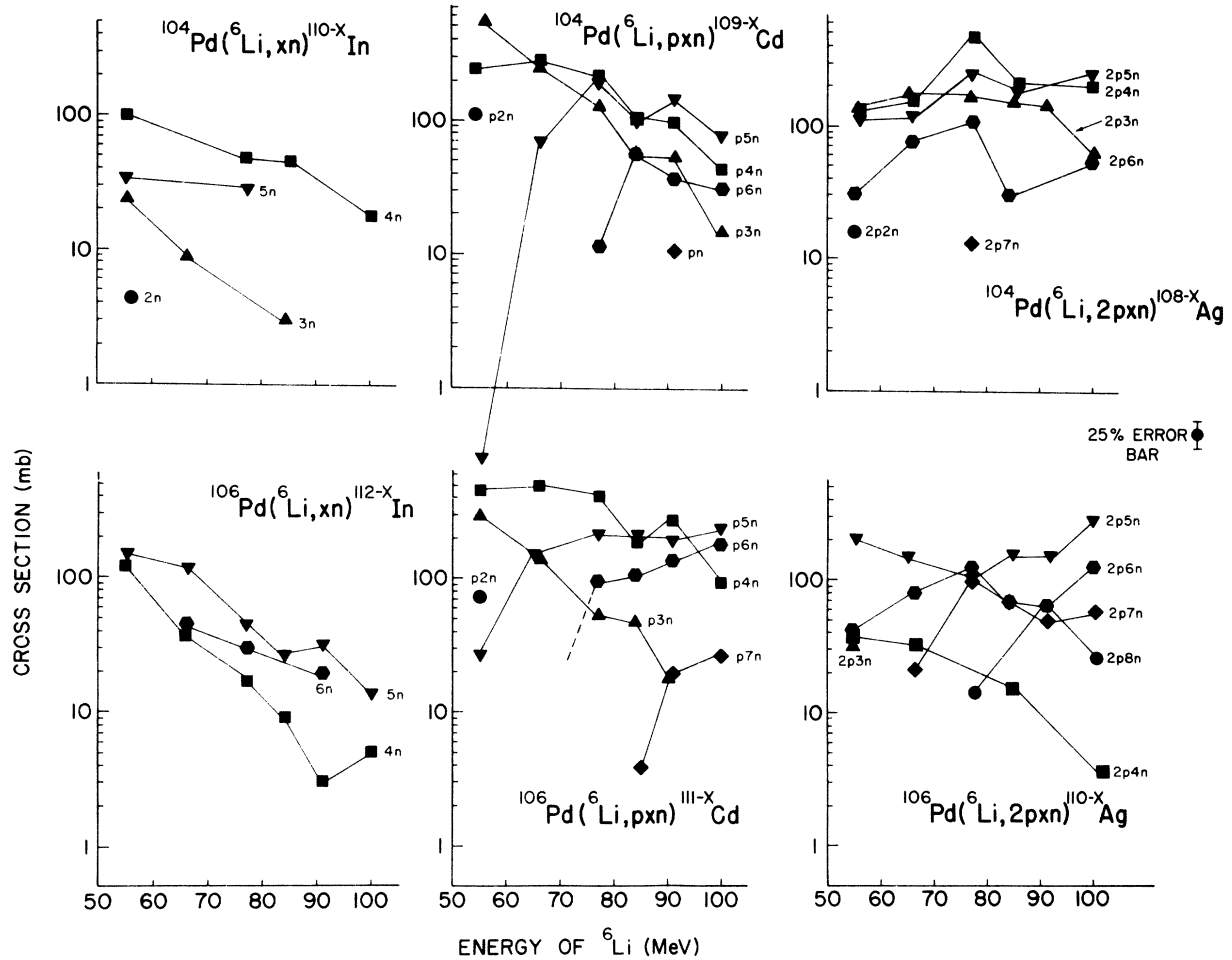


FIG. 2. Experimental excitation functions for ${}^6\text{Li}$ -induced reactions on ${}^{104}\text{Pd}$ (upper plots) and ${}^{106}\text{Pd}$ (lower plots). Cross sections are quoted with a 25% uncertainty, and the lines are drawn solely as a guide to the eye. For purposes of discussion, the cross sections are labeled solely by the values of x and y in the " $({}^6\text{Li}, xny p)$ " designation of the reaction; although, as discussed in the text, this designation may not always be completely appropriate.

mechanism but also involve pre-equilibrium emission of nucleons during the course of the reactions. Excitation functions calculated from a simple fusion-evaporation model and those resulting from processes which also involve pre-equilibrium emission will differ most dramatically in the high-energy tails for reaction products close to the compound nucleus in mass. In Fig. 3 we show the measured excitation functions for the production of ${}^{109}\text{In}$ and ${}^{108}\text{Cd}$ by the $({}^6\text{Li}, 4n)$ and the $({}^6\text{Li}, p3n)$ reactions on ${}^{106}\text{Pd}$, and the data are compared with the predictions based on the GDHM calculation (solid curves) and an alternate calculation involving only the fusion-evaporation mechanism (dashed curves). The data clearly indicate the need to include pre-equilibrium emission processes in the description of ${}^6\text{Li}$ -induced reactions in the energy range above 50 MeV. (The normalization of the calculations indicated in the figure

will be discussed in subsequent sections.) In the discussion to follow, the term "fusion-emission" will be used to designate the combination of fusion-evaporation and pre-equilibrium emission reaction mechanisms into a single reaction concept.

One other way to view the behavior of these reactions is to consider the energy dependence of the average number of nucleons, $\langle \Delta A \rangle$, emitted by the compound system. This number is defined as the cross-section-weighted average of the number of nucleons emitted in each observed process and is given by:

$$\langle \Delta A \rangle = \frac{\sum_{x,y} (x+y) \sigma({}^6\text{Li}, xny p)}{\sum_{x,y} \sigma({}^6\text{Li}, xny p)}, \quad (1)$$

where the indices summed over represent all of the final reaction products at each beam energy.

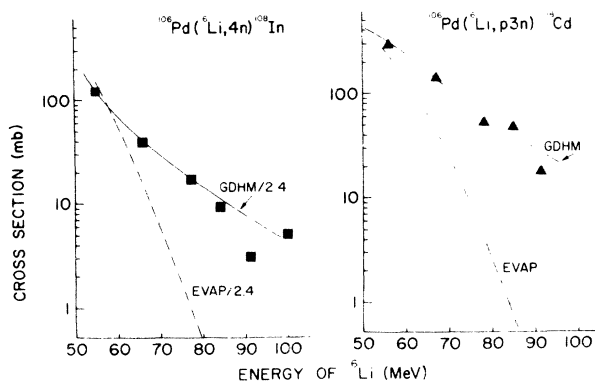


FIG. 3. Comparison of measured $^{106}\text{Pd}(^6\text{Li}, 4n)$ and $^{106}\text{Pd}(^6\text{Li}, p3n)$ excitation functions with theoretical predictions based upon a simple fusion-evaporation model (dashed curve) and the GDHM calculation, including pre-equilibrium emission (solid curve). For a discussion of the normalization of the GDHM calculations, see text.

The experimental determination of this number at the five beam energies used is presented in Fig. 4. (The experimental points were obtained from the data in Table II, and appropriate interpolations of the data were made where necessary.) It is clear from the figure that over the 45-MeV beam energy range, the quantity $\langle\Delta A\rangle$ varies by only 1.5 units, or exhibits a slope of 0.03 nucleon/MeV added energy. Normally, a pure fusion-evaporation mechanism would give rise to a slope of approximately 0.1 nucleons/MeV, and so the present results suggest that very little of the additional beam energy goes into internal excitation of the compound (equilibrated) system. Instead, it seems that much of the extra energy is shared by only a few nucleons, resulting in increases high-energy nucleon emission prior to equilibration.

The GDHM prediction of the quantity $\langle\Delta A\rangle$ is also shown in Fig. 4, and the general agreement

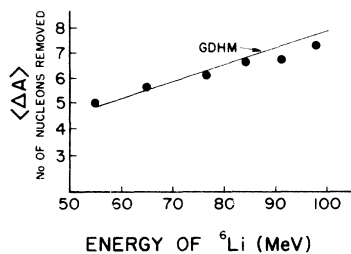


FIG. 4. Energy dependence of the cross-section-weighted average of the number of nucleons emitted in the ^6Li -induced reactions on ^{106}Pd . The slight deficiency in the measured value of this quantity at the high Li energies can be attributed to the exclusion of the Pd production in the data analysis. (See discussion in text in reference to Fig. 5.)

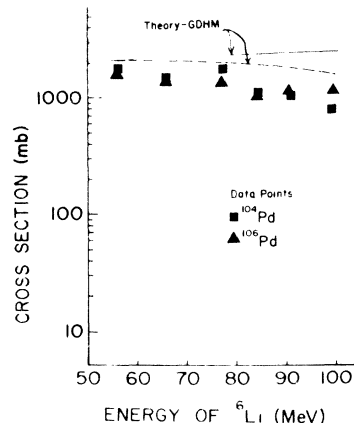


FIG. 5. Total ^6Li compound-nucleus formation cross section as a function of beam energy for $^{104}, ^{106}\text{Pd}$ targets. The theoretical curves represent the optical model predictions of this quantity, as provided in the GDHM calculation (Ref. 5). The solid curve represents the complete fusion reaction cross section, and the dashed curve shows the fusion cross section excluding the Pd production [the $(3p3n)$ exit channel].

of the calculation with the data is evident. The calculation, as applied in the present study, assumes a single pre-equilibrium nucleon emission in the initial process of equilibration. The general agreement shown in Fig. 4, therefore, strongly suggests that for ^6Li -induced reactions in this energy range, this assumption is reasonable. This is in contrast to results obtained by Sadler *et al.*,¹⁵ who investigated intermediate-energy proton-induced nucleon removal with $^{58,62}\text{Ni}$ targets. These authors found that the observed number of nucleons removed at all beam energies used was lower than that predicted by the GDHM calculation under the assumption of a single pre-equilibrium emission. By including *multiple* pre-equilibrium emission, these authors were successful in explaining the observed energy dependence of the average number of nucleons removed. The fact that the original single pre-equilibrium emission assumption works reasonably well in the present case studied here suggests that the larger number of excitons brought into the complex system by the ^6Li projectile dissipates the excitation energy more quickly leaving less chance for more than one pre-equilibrium emission in the process of equilibration.

The total reaction cross sections observed in the present measurements on both targets are plotted in Fig. 5 *versus* ^6Li beam energy and are compared with the values calculated by means of the optical model, as applied in the GDHM calculation.⁵ As before, the data for this plot were obtained from Table II, and interpolations of the

observed results were made where necessary. The increase in the discrepancy between theory and experiment at the higher energies may be due in part, to the incipient production of Pd isotopes at the higher ${}^6\text{Li}$ energies. These isotopes were not easily observed since many of these products (${}^{102-106}\text{Pd}$) are stable or very long-lived, and in-beam Pd γ rays from high-spin states are also produced by the short-lived decays from high-spin states in the Ag isotopes. The dashed curve of Fig. 5 shows the optical model predictions for the total cross section if the Pd production is ignored (as was essentially the case in this experiment). It should be noted that if the missing observed cross section were due to the production of unobserved neutron-deficient products, then the discrepancy between the optical model prediction and the experimental result should be greater for the ${}^{104}\text{Pd}$ bombardment than for that of ${}^{106}\text{Pd}$. The data shown in Fig. 5, however, do not exhibit any significant differences between the ${}^{104}\text{Pd}$ and ${}^{106}\text{Pd}$ cross sections, and so we conclude that the major contribution to the energy dependence of the discrepancy in question arises from the Pd production by $({}^6\text{Li}, 3p xn)$ reactions which were not analyzed in the present investigation. [It should also be noted that reaction products resulting from direct transfer processes, such as $({}^6\text{Li}, d)$ or $({}^6\text{Li}, \alpha)$, were not seen, usually because the residual nucleus was either stable or a long-lived product whose decay could not be observed easily.]

It is evident from Fig. 5 that the total observed production cross section is consistently below the total reaction cross section which is predicted by the optical model, even at the lowest beam energies utilized. While it might be argued that direct reactions to stable nuclides can account for some of this discrepancy, our data, when considered in somewhat more detail, suggest other possible mechanisms as well. In Fig. 6 are shown the total ${}^{106}\text{Pd}({}^6\text{Li}, xn)$ and ${}^{106}\text{Pd}({}^6\text{Li}, p xn)$ yields observed in this experiment at each ${}^6\text{Li}$ energy, and comparison is made with the GDHM calculation for these same integrated yields. The most striking feature of this figure is the large *systematic* overestimate of the $({}^6\text{Li}, xn)$ yields by the GDHM calculations for ${}^6\text{Li}$ -induced reactions. By contrast, the $({}^6\text{Li}, p xn)$ yields are not as severely overestimated. The overall normalization of the GDHM calculation may possess some systematic error due to uncertainties in the nucleon-nucleon interaction matrix elements, but predictions of the *relative isotopic* yields at a given beam energy should be reliable. Thus, the fact that the discrepancy between predicted and observed (xn) yields is much greater than that for the $(p xn)$ yields suggests that another

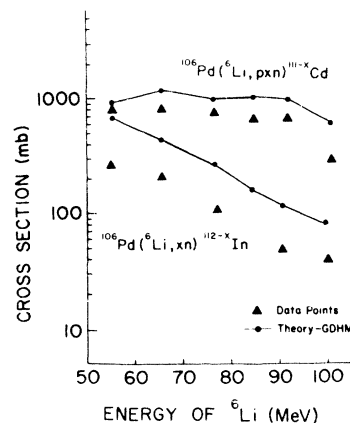


FIG. 6. Total measured indium [($p xn$) exit channel] and cadmium [($p xn$) exit channel] yields from ${}^6\text{Li}$ bombardment of ${}^{106}\text{Pd}$ versus beam energy. Comparison with the predictions of the GDHM calculations are also provided (Ref. 5).

reaction mechanism may be providing additional cross sections in what appears to be the charged-particle emission channels. [The Ag($2p xn$) yields also show some deficiency with respect to the GDHM calculation; but, as with the $(p xn)$ yields, this deficiency is not clearly as great as that seen in the (xn) yields.]

One plausible mechanism by which such behavior could occur involves the binary breakup of the ${}^6\text{Li}$ projectile, either in advance of or during the reaction. Early experiments with ${}^6\text{Li}$ established that this nucleus has a well-developed cluster structure with significant α - d amplitude¹⁶⁻²⁰ and also ${}^3\text{He}$ - t amplitude.²¹ Some studies of ${}^7\text{Li}$ cluster structure have also been carried out.^{17,22,23} The high degree of clustering in the ${}^6\text{Li}$ ground states implies a significant probability that, when used as projectiles, these nuclei will often undergo binary dissociation into their cluster substructures. This observation has in fact led to the use of Li ions in cluster transfer studies, particularly those investigating α transfer.²⁴⁻²⁶ In addition, a number of experimental^{22,23,27,29} and theoretical³⁰⁻³⁵ studies of the lithium breakup phenomenon itself have been carried out. Up to now these works have been confined to Li projectile energies at or near the Li-nucleus Coulomb barriers, where the general conclusion is that the Li breakup is largely Coulomb induced, with some influence from the "tails" of the nuclear potential.³⁰ At the higher Li energies (in the neighborhood of 100 MeV) the mechanism and extent of both the Li breakup and cluster transfers may be very different from that experienced at near-barrier energies. For example, it is reasonable to expect that the nuclear force will play a more prominent role in the breakup mechanism as the projectile energy in-

creases. This would have important bearing on all experiments which utilize Li projectiles at higher energies. If a significant prereaction breakup of the ${}^6\text{Li}$ occurs, this could account for a large part of the apparent loss of ${}^6\text{Li}$ fusion-emission cross section observed in the present measurements. In order to confirm this possibility, quantitative charged-particle spectrum measurements must be made, and such measurements are currently under way at this laboratory. Some preliminary measurements pertaining to this question were performed during the course of this investigation, and a portion of those results is shown in Fig. 7. A number of targets, ranging in Z from 6 to 83 and including ${}^{106}\text{Pd}$, were bombarded with 91-MeV ${}^6\text{Li}$; and selected charged-particle spectra were observed at 25° in the laboratory with a silicon two-detector (200- μm ΔE and 3500- μm $E-\Delta E$) telescope. The spectra in Figs. 7(a), 7(b), and 7(c) are those of all charged particles, α particles, and $Z=1$ particles, respectively. A two-parameter analysis of the ΔE and the $E-\Delta E$ signals showed a large number of α particles and a negligible number of ${}^3\text{He}$ particles at 25° . On the other hand, the same analysis showed the central group in Fig. 7(c) to be the deuterons observed and the accompanying groups on the high- and low-energy side of the deuterons

to be tritons and protons, respectively. As is evident from Fig. 7, a significant number of α particles and deuterons were observed which exhibit energies that are concentrated around values consistent with the beam velocity. This observation suggests that a number of ${}^6\text{Li}$ α - d breakup fragments are present and may be an indication of the primary mechanism by which the total reaction cross section is partially diverted to outgoing channels other than isotope production by ${}^6\text{Li}$ -target fusion. Quantitative analysis of these preliminary charged-particle spectra is difficult, as these data were actually acquired in order to test some experimental apparatus. However, very rough estimates of the appropriate quantities and integration of the α -particle spectrum gives an approximate estimate of the α - d breakup cross section of several hundred millibarns for the ${}^6\text{Li}$ bombardment of palladium.

The observed diminutive yield of ${}^3\text{He}$ particles in the $Z=2$ spectrum at 25° may seem at first surprising in view of both the ${}^3\text{He}$ - t cluster structure which is believed to be in the ${}^6\text{Li}$ ground state²¹ and our observation of significant numbers of tritons. However, this result may only be the consequence of a less-than-optimum choice of detector angle for observation of this particular particle. The question of the presence or absence

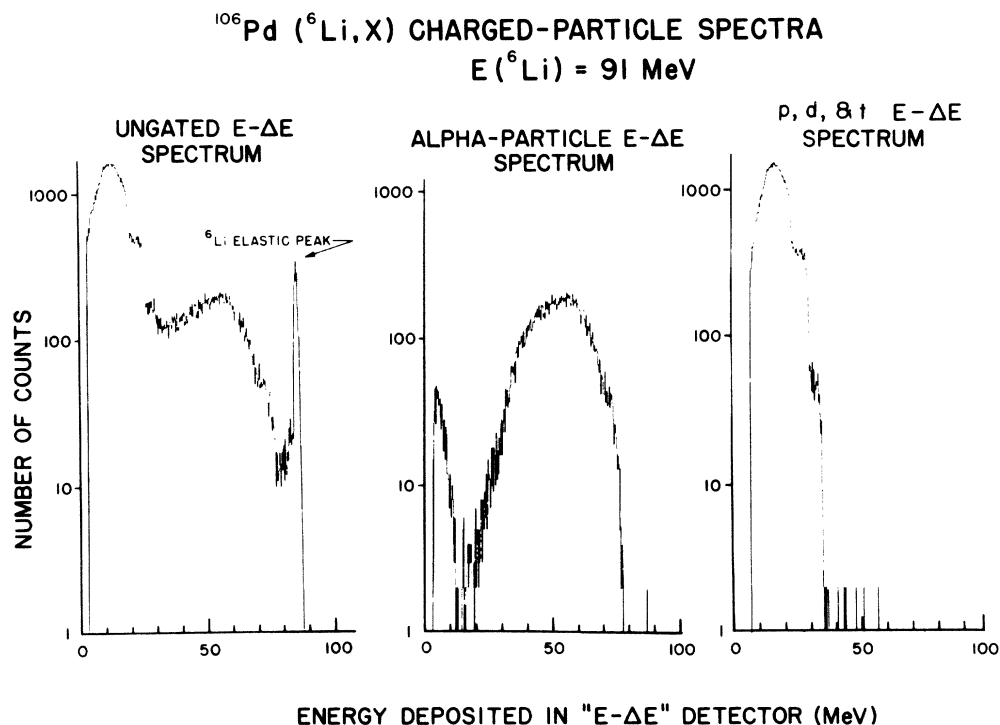


FIG. 7. Data from preliminary measurements of charged-particle spectra resulting from 91-MeV ${}^6\text{Li}$ bombardment of ${}^{106}\text{Pd}$. Shown are the $E-\Delta E$ spectra for (a) all charged particles, (b) α particles, and (c) $Z=1$ particles. In the last group the deuterons comprise the central "shoulder" in the spectrum shown.

of ${}^3\text{He}$ - t fragments in the ${}^6\text{Li}$ reactions will be addressed more carefully in subsequent experiments at this laboratory.

The data shown in Fig. 8 depict the isotopic yields from ${}^6\text{Li}$ bombardment of ${}^{104}\text{Pd}$ at 54 MeV and suggest the existence of a possible reaction mechanism accompanying a ${}^6\text{Li}$ breakup and, of course, another source of the α and d fragments seen in our preliminary charged-particle measurements. In this figure we compare the observed yields with the predictions of the GDHM calculations for total absorption of the ${}^6\text{Li}$ (solid lines). The ${}^6\text{Li}$ GDHM calculations were normalized to the $({}^6\text{Li}, xn)$ yields in the spirit that these reactions represent the extent to which the Li-target fusion mechanism is present. The Ag yields occasionally exhibit large discrepancies of the type shown in the figure, where a dramatic excess of cross section can be seen in the $(2p4n)$ exit channel. [For purposes of discussion, the isotopic yields are designated by the $({}^6\text{Li}, xpy_n)$ reaction which would produce them, even though this particular reaction may not always be the dominant mode by which the isotope is produced.] In this particular case, the (d, yn) and (α, pz_n) reactions, where the α and

d are incident with the 54-MeV ${}^6\text{Li}$ beam velocity, are predicted by the GDHM calculations to exhibit cross sections which peak strongly in the $(d, 2n)$ and $(\alpha, p3n)$ channels. This is depicted by the dotted curves in Fig. 8, where the (α, xn) production of the Cd isotopes at the beam velocity is also shown. Such a calculation can be interpreted as a theoretical simulation of the scattering by the target nucleus of one of the ${}^6\text{Li}$ fragments, accompanied by the (complementary fragment, xn or pxn) reactions. Thus our data, interpreted in this way, suggest the occurrence of occasional breakup of the ${}^6\text{Li}$ in the nuclear field and the retention of one of the fragments by the residual nuclear system. In the case of the Ag yields shown in Fig. 8, this would mean that fusion of the target and deuteron is providing the excess cross section observed. A similar result for the 54-MeV bombardment of ${}^{106}\text{Pd}$ is shown in Fig. 9, where the discrepancy in the Ag yield is also explained by the presence of a (d, xn) process.

The theoretical predictions for the fragment-induced and ${}^6\text{Li}$ -induced cadmium production [the (pxn) exit channel] are generally similar enough when viewed as mass yields that the experimental

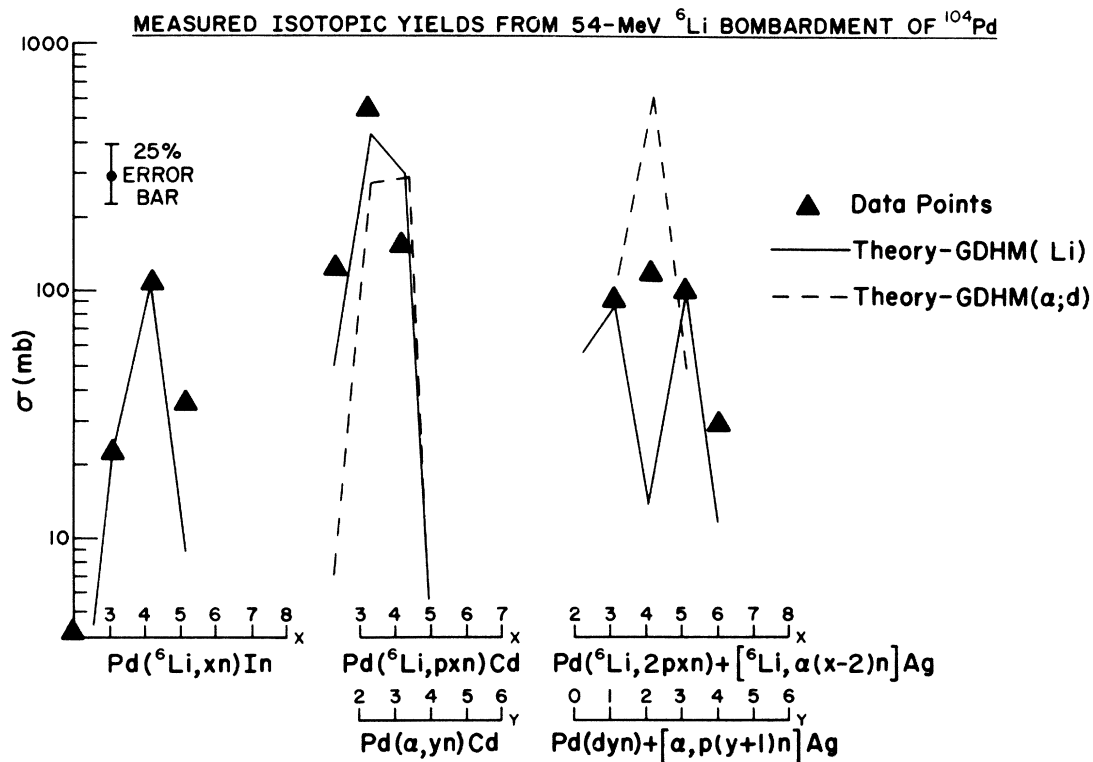


FIG. 8. Isotopic yields from 54-MeV ${}^6\text{Li}$ bombardment of ${}^{104}\text{Pd}$. The ${}^6\text{Li}$ -induced GDHM calculation (solid line) has been normalized to the $({}^6\text{Li}, xn)$ yields, and no renormalization of the calculated fragment-induced yields (dotted lines) was performed. These latter yields are calculated from (d, xn) , (α, xn) , and (α, pxn) reactions on the target, the incident particles being given kinetic energies corresponding to the ${}^6\text{Li}$ beam velocity.

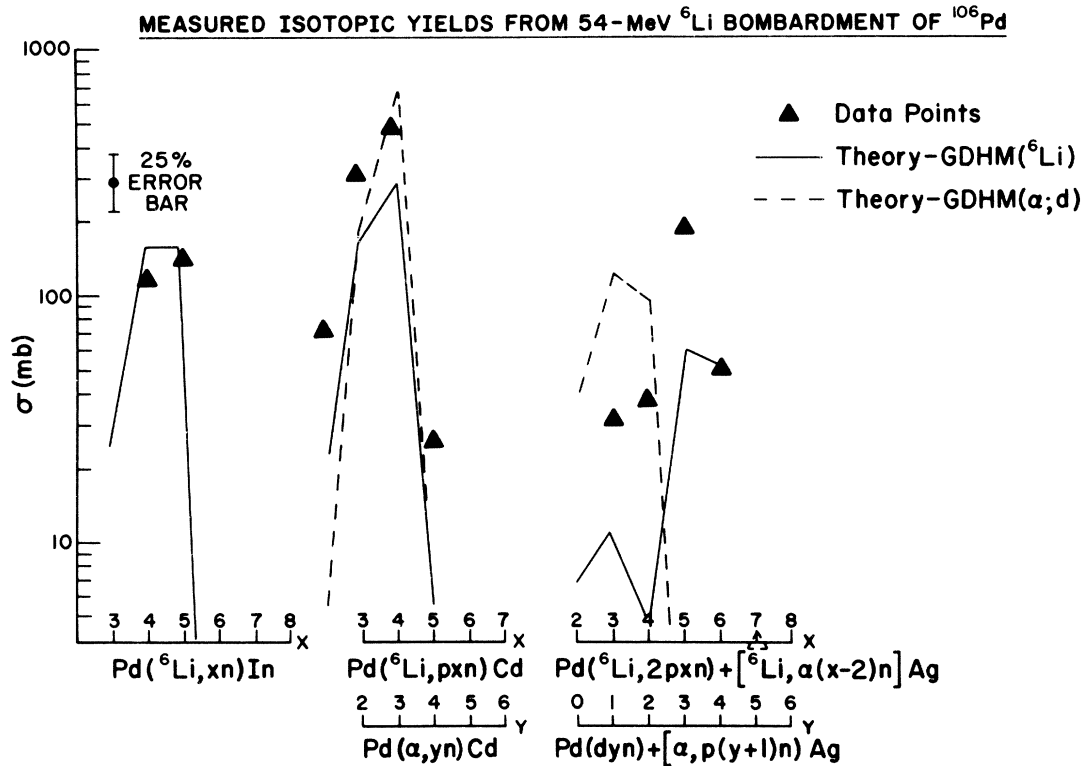


FIG. 9. Same as Fig. 8, but for the ${}^{106}\text{Pd}$ target.

data cannot distinguish between the two processes. It is, however, plausible that if the experimental (${}^6\text{Li}, xn$) yields are attenuated relative to the optical model prediction, the (${}^6\text{Li}, pxn$) and (${}^6\text{Li}, 2pxn$) reactions should be similarly reduced. The fact that the Cd and Ag yields are not as attenuated as the In yields, coupled with the theoretical predictions for fragment-induced reactions shown in Figs. 8 and 9, suggest that the α - d breakup of the ${}^6\text{Li}$, followed by fusion-emission reactions from one of the lithium fragments, could replace much of what would be missing cross section in the Cd and Ag production channels. Furthermore, in the few isolated cases where the ${}^6\text{Li}$ -fusion and the fragment-fusion GDHM calculations do not predict similar results, the data show strong disagreement with the ${}^6\text{Li}$ -induced GDHM calculation, and this discrepancy is resolved by allowing a small contribution from a fragment-induced reaction where the incident fragment is given the same velocity as the incident ${}^6\text{Li}$ beam.

Similar conclusions have been reached in a recent study by Kropp, *et al.*,³⁸ who performed ${}^6\text{Li}$ bombardments in the Au region. These authors see strong evidence for a breakup mechanism and speculate that an observed excess of cross section in the charged-particle emission channels of the

(${}^6\text{Li}, xny$) reaction is contributed by fragment-induced reactions on the target nucleus. In addition, recent excitation function studies at this laboratory by Fleissner *et al.* on rare-earth targets³⁹ and by Tickle *et al.* on a ${}^{209}\text{Bi}$ target⁴⁰ have revealed an excess of cross section in the (pxn) and ($2pxn$) exit channels compared with that predicted by GDHM calculations normalized to observed (xn) yields. Furthermore, Fleissner *et al.*³⁹ have shown that the experimental mass yields for both the (pxn) and ($2pxn$) exit channels peak at masses consistent with a strong contribution from the fragment-induced mechanism and not at masses predicted for fusion of the ${}^6\text{Li}$ projectile and target nucleus.

IV. CONCLUSION

The present measurements provide a reasonably complete picture of the gross features of the isotope production derived from ${}^6\text{Li}$ bombardment of ${}^{104,106}\text{Pd}$ at energies from 54 to 99 MeV. The data show that pre-equilibrium nucleon emission is important but probably involves a single rather than multiple nucleon emission. More detailed

consideration of the isotopic yields suggests that reactions resulting from the breakup of the ${}^6\text{Li}$ projectile may be contributing to the total reaction cross section. In particular, we have shown evidence that breakup of the ${}^6\text{Li}$, accompanied by the absorption by the target of one of the fragments, is likely to be occurring with significant cross section. Further studies of this latter phenomenon are planned, and these investigations will involve the explicit observation of correlated charged-particle and γ -ray spectra.

V. ACKNOWLEDGMENTS

The authors would like to express their appreciation to the IUCF operating crew for their cooperation in all of the bombardments and to Mr. G. S. Adams and Mr. W. Lozowski for preparation of the ${}^6\text{Li}$ sources and target foils, respectively. We also extend our thanks to Professor Marshall Blann for providing both a copy of his computer code of the GDHM calculations and some helpful discussions.

-
- ¹H. A. Smith, Jr., C. M. Castaneda, T. R. Nees, T. E. Ward, and E. S. Macias, *Bull. Am. Phys. Soc.* **21**, 1005 (1976).
- ²R. Kouzes and A. Broad, IUCF Internal Report No. 75-6, April, 1976 (unpublished).
- ³C. Cline and M. Blann, *Nucl. Phys.* **A172**, 225 (1971).
- ⁴M. Blann, *Annu. Rev. Nucl. Sci.* **25**, 123 (1975); and Univ. of Rochester Report No. COO-3494-13 1974 (unpublished).
- ⁵Code ALICE OVERLAID, M. Blann, Univ. of Rochester Report No. COO-3494-29, 1976 (unpublished).
- ⁶M. Blann, *Phys. Rev. Lett.* **27**, 337 (1971).
- ⁷M. Blann and A. Mignerey, *Nucl. Phys.* **A186**, 245 (1972).
- ⁸J. J. Griffin, *Phys. Rev. Lett.* **17**, 478 (1966).
- ⁹G. D. Harp, J. M. Miller, and B. J. Berne, *Phys. Rev.* **165**, 1166 (1968).
- ¹⁰G. D. Harp and J. M. Miller, *Phys. Rev. C* **3**, 1847 (1971).
- ¹¹M. Blann, *Phys. Rev. Lett.* **28**, 757 (1972).
- ¹²S. M. Grimes, J. D. Anderson, J. C. Davis, and C. Wong, *Phys. Rev. C* **8**, 1770 (1973).
- ¹³M. Blann and G. Merkel, *Phys. Rev.* **137**, B367 (1965).
- ¹⁴T. Ericson, *Advan. Phys.* **9**, 425 (1960).
- ¹⁵M. E. Sadler, P. P. Singh, R. E. Segel, L. Rutledge, and J. Jastrzebski, *Bull. Am. Phys. Soc.* **22**, 562 (1977); and IUCF Technical and Scientific report, 1977 (unpublished), p. 69.
- ¹⁶G. C. Morrison, *Phys. Rev. Lett.* **5**, 565 (1960).
- ¹⁷R. W. Ollerhead, C. Chasman, and D. A. Bromley, *Phys. Rev.* **134**, B74 (1964).
- ¹⁸J. R. Pizzi, M. Gaillard, P. Gaillard, A. Guichard, M. Gusakow, G. Reboulet, and C. Ruhler, *Nucl. Phys.* **A136**, 496 (1969).
- ¹⁹J. W. Watson, H. G. Pugh, P. G. Roos, D. A. Goldberg, R. A. J. Riddle, and D. I. Bonbright, *Nucl. Phys.* **A172**, 513 (1971).
- ²⁰A. K. Jain, J. Y. Grossiard, M. Chevallier, P. Gaillard, A. Guichard, M. Gusakow, and J. R. Pizzi, *Nucl. Phys.* **A216**, 519 (1973).
- ²¹D. Bachelier, M. Bernas, C. Detraz, P. Radvanyi, and M. Roy, *Phys. Lett.* **26B**, 283 (1968).
- ²²O. Häuser, A. B. McDonald, T. K. Alexander, A. J. Ferguson, and R. E. Warner, *Phys. Lett.* **38B**, 75 (1972).
- ²³J. L. Quebert, B. Frois, L. Marquez, G. Sousbie, R. Ost, K. Bethge, and G. Gruber, *Phys. Rev. Lett.* **32**, 1136 (1974).
- ²⁴K. P. Artemov, V. Z. Goldberg, I. P. Petrov, V. P. Rudakov, I. N. Serikov, and V. A. Timofeev, *Yad. Fiz.* **21**, 1157 (1975) [*Sov. J. Nucl. Phys.* **21**, 596 (1976)].
- ²⁵M. E. Cobern, D. J. Pisano, and P. D. Parker, *Phys. Rev. C* **14**, 491 (1976).
- ²⁶G. E. Moore and K. W. Kemper, *Phys. Rev. C* **14**, 977 (1976).
- ²⁷R. Ost, E. Speth, K. O. Pfeiffer, and K. Bethge, *Phys. Rev. C* **5**, 1835 (1972).
- ²⁸K. O. Pfeiffer, E. Speth, and K. Bethge, *Nucl. Phys.* **A206**, 545 (1973).
- ²⁹D. L. Disdier, G. C. Ball, O. Häusser, and R. E. Warner, *Phys. Rev. Lett.* **27**, 1391 (1971).
- ³⁰J. M. Hansteen and H. Wittern, *Phys. Rev.* **134**, B524 (1965); *Z. Phys.* **183**, 447 (1965).
- ³¹H. Wittern, *Z. Forsch. Phys.* **14**, 401 (1966).
- ³²K. Bethge and K. Meier-Ewert, *Phys. Rev. Lett.* **18**, 1010 (1967).
- ³³H. Wittern, *Phys. Lett.* **32B**, 441 (1970).
- ³⁴A. A. Oglobin, *Fiz. Elem. Chast. At. Yad.* **3**, 936 (1972) [*Sov. J. Part. Nucl.* **3**, 467 (1973)].
- ³⁵A. I. Titov, *Yad. Fiz.* **19**, 292 (1974) [*Sov. J. Nucl. Phys.* **19**, 143 (1974)].
- ³⁶F. A. Rickey *et al.* (private communication).
- ³⁷R. E. Anderson, B. L. Bunting, J. D. Burch, S. R. Chinn, J. J. Kraushaar, R. J. Peterson, D. E. Prull, B. W. Ridley, and R. A. Ristinen, *Nucl. Phys.* **A242**, 93 (1975).
- ³⁸J. Kropp, H. Klewe-Nebenius, H. Faust, J. Bushman, H. Rebel, H. J. Gils, and K. Wisshak, *Z. Phys.* **A280**, 61 (1977).
- ³⁹J. Fleissner, D. Rakel, F. Venezia, S. Rozak, E. G. Funk, J. W. Mihelich, and H. A. Smith, Jr., *Bull. Am. Phys. Soc.* **21**, 1006 (1976); and IUCF Technical and Scientific report, 1977 (unpublished), p. 87.
- ⁴⁰R. S. Tickle, H. C. Griffin, W. S. Gray, and H. Smith, *Bull. Am. Phys. Soc.* **22**, 643 (1977); and IUCF Technical and Scientific Report, 1977 (unpublished), p. 85.